

Supplementary information

Friction-Directed Self-Assembly of Janus Lithographic Micogels into Anisotropic 2D Structures

Yadu Nath Vakkipurath Kodakkadan,^a Charlie Maslen,^a Petr Cigler,^b Frantisek Stepanek,^a Ivan Rehor^{*a,b}

^a University of Chemistry and Technology Prague, Faculty of Chemical Engineering, Technicka 5, 166 28 Prague 6, Czech Republic

^b Institute of Organic Chemistry and Biochemistry of the Czech Academy of Sciences, Flemingovo nam. 2, 160 00, Prague, Czech Republic

* e-mail: ivan.rehor@vscht.cz

Supplementary text S1:

Sliding at various angles:

At the tilt angles 3°, 6°, and 9°, the reorientation occurred over a traveled distance corresponding to several microgel diameters, while at 12° the reorientation took more distance and time. Furthermore, we observed different equilibrium angles of sliding hexagonal microgels at 12° – instead of sliding the PEGDA side first, they slide tilted by 60° with respect to this position (Fig. S3). Apparently, new phenomena are participating under the high tilt angle. We hypothesize these may originate from non-perfectly flat microgels (The PEGDA side is somewhat thicker ~1-2 μm due to somewhat higher photo-reactivity of the PEGDA pregel compared to the PNIPAM pregel¹) which causes mild tilt of the hydrogel and so can generate lift force². However, for the angles 10° and below, the microgels self-orientate the PEGDA side down the slope.

Supplementary text S2:

Self-orientation rates of Janus hydrogels of different shapes

The rate of self-orientation of a microgel depends on the torque, given by the separation between the center of mass and the center of friction. Both microgels are of very similar density and, thus we assume the center of mass to be at the geometrical center of the polygon. The center of friction for a sheared plane, composed from a single material will be identical to the center of mass, as we state in the main text. Hence, to find the center of friction of the whole polygon, we first calculate the distance (d) between the center of friction/mass of the half of the polygon of uniform composition and the geometrical center/center of mass of the whole polygon. The distance between the center of friction of the whole Janus microgel and its center of mass (δ) can be calculated from these two uniform-composition centers in an analogy to the center of mass.

$$\delta = d \cdot \left(f_1 + \frac{f_2}{f_1} \right) + f_2 \quad (\text{S1})$$

Where f_1 and f_2 are friction forces of the respective halves of the microgel. Since the material compositions are constant (PEGDA and PNIPAM, respectively) and the polygons and the sheared areas are identical, the f_1 and f_2 are constant and the only variable in the equation is d . The larger is the d , i.e. the longer the particle in the direction perpendicular to the interphase boundary, the greater is the difference between the center of mass and the center of friction, which ultimately results in greater torque.

All values below are derived using simple geometrical principles and thus the derivations are not shown in detail. For a regular hexagon of an edge length a , the distance d is $\frac{7}{18}a$ ($0.389a$). An isoareal square to the hexagon of an edge a has edge length b

equal to $\sqrt{3} \cdot \left(\frac{\sqrt{3}}{2}\right) \cdot a$. The distance between the center of mass and the center of mass of half of such square, divided along its diagonal is equal to $\frac{1}{3\sqrt{2}} \cdot b$ which corresponds to approximately $0.379a$. Since the lower d results in the lower mass δ and, ultimately, in lower torque, the square is expected to rotate slower, than the hexagon. For isoareal rhombus, the d is equal to $0.289a$, which, as shown in the sliding experiments, is not sufficient separation to achieve a self-orientation. On the other hand, for the elongated hexagon (two parallel edges have double-length; all angles are equal to 120°) the d is $0.838a$ and these hexagons rapidly self-oriented in conducted experiments.

Supplementary text S3:

Self-assembly of Janus hexagons of various sizes

We were also interested in the SA behavior of hexagons of other sizes. Particles larger than $200 \mu\text{m}$ (and identical height $30 \mu\text{m}$) tended to stick to the surface during sliding, which hindered the SA process. We currently have no explanation for this emergence of the static friction with a mere increase of the microgel lateral dimensions. Platelets with lateral dimensions below $50 \mu\text{m}$ tended to sediment on their edges (being $30 \mu\text{m}$ high), which again hindered the SA process. This could be overcome by synthesizing thinner microgels, but these exhibit tendency to slide over each other and form multilayered structures instead of single layer tiles.

Supplementary text S4:

Self-assembly of concave Janus microgels

We studied the impact of a concave region on the self-assembly process by designing arrow-shaped microgels with a convex corner on the slippery side and a complementary concave region on the opposite side. The arrows formed interlocked chains during the sliding phase (Fig. S7a, video S8). This phenomenon originates from non-uniform sliding velocities of the individual microgels – when the faster microgel reaches the slower one, they interlock and continue as a chain. The variation in microgels' sliding speeds originates from their synthesis. The position of the PEGDA-PNIPAM pregel boundary would oscillate somewhat during the microfluidic fabrication, which resulted in variable PEGDA-PNIPAM gel ratio in each microgel particle and ultimately in variation in their sliding speeds. Naturally, the microgel chains collapsed at the bottom of the well forming a random assembly (Fig. S7b).

Supplementary text S4:

Anisotropically actuating sheets

In the next section of this work, we show a potential way to use the demonstrated assembling system for the fabrication of 2D micropatterned soft materials. The microgels in selected areas of the self-assembly can be bound covalently together into a single sheet using remnant acrylate moieties present in the hydrogel. A similar methodology has been previously used for covalent binding of acrylate microgels^{3,4}. The microgels are composed of PNIPAM, crosslinked with PEGDA and pure PEGDA respectively. Some of the PEGDA molecules are incorporated into only a single polymeric chain during the microgel synthesis and, thus, contain one unreacted acrylate moiety which can be used for the covalent binding. To perform the reaction, LAP photoinitiator was added to the well and the assembly was irradiated with UV light to initiate radical polymerization of the remnant acrylates. These remnant acrylates come from either two adjacent microgels, which results in the discs binding or, alternatively, they are present within a single microgel and the newly formed, internal, crosslinks densify the hydrogel network, which results in isotropic shrinkage of the microgel⁵. Both these processes occur simultaneously, so the microgels bind into a single sheet while their linear dimensions reduce by ~20 %.

The resulting sheet is composed of spatially organized segments of PEGDA and PNIPAM respectively. Since the PNIPAM is thermoresponsive, these segments will undergo isotropic shrinkage upon heating while the PEGDA ones will keep constant volume. As a result, the entire sheet will shrink anisotropically, given by the spatial arrangement of the respective segments. The non-responsive PEGDA sections are connected into stripes, which are responsible for lower shrinkage in the direction parallel to these ribbons, than the perpendicular one. Indeed, we observed anisotropic shrinkage rates in the perpendicular directions of the sheet, subjected to heating-cooling (Fig. S8). This experiment indicates the potential future application of micropatterned sheets in microscale actuation, however, it will require a theoretical understanding of the mechanics of the process to gain predictive power over the programming of the anisotropic response through designing of the building block shapes

Supplementary figures:

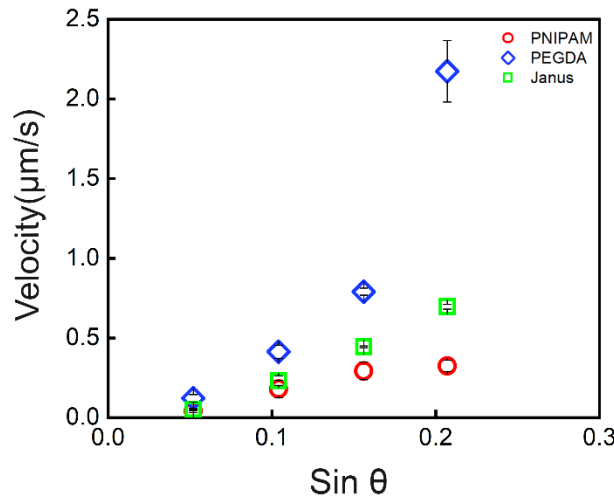


Fig. S1. Sliding velocities of microgels, composed from single-phase PNIPAM (circles) and PEGDA (diamonds) hydrogel, and Janus PNIPAM-PEGDA microgels (squares) at angles 3°, 6°, 9°, and 12° respectively. We ascribe the intercept present at the x axis (the zero velocity would correspond to the tilt angle around 2°) to a static friction contribution. The error bars represent the standard deviation from 10 experiments.

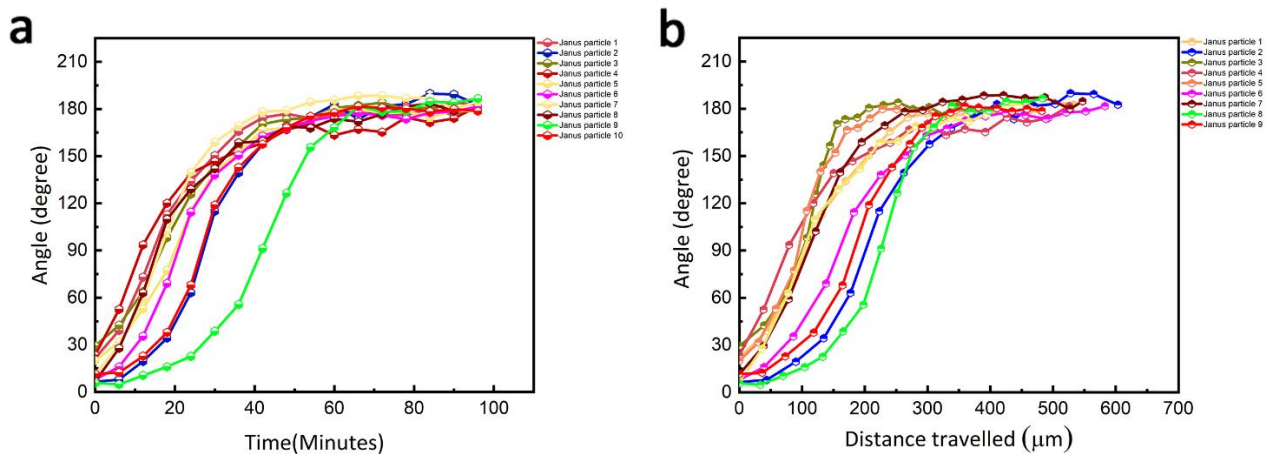


Fig. S2. Reorientation of Janus hexagons at 6° tilt as a function of a. Time, b. Traveled distance, respectively. To observe the orientation change in the entire 180° range, the hexagons were preoriented by tilting the well in the opposite direction.

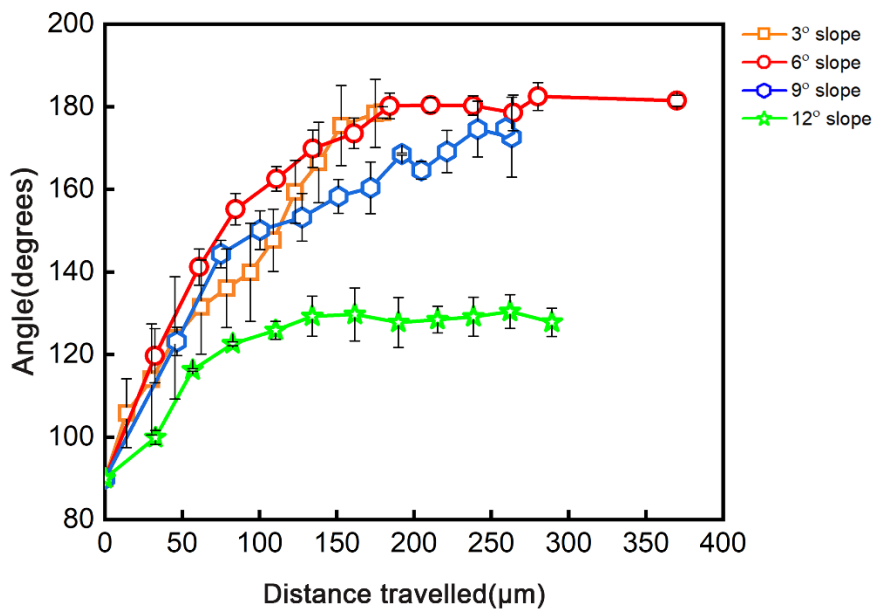


Fig. S3. Sliding hexagons – images show gradual alignment of the Janus hexagons on a 3° (orange rectangle), 6° (red circle), 9° (blue hexagon), 12° (green star) slopes. Only the second half of the reorientation is plotted, i.e. the initial orientation of the Janus boundary is parallel to the sliding direction.

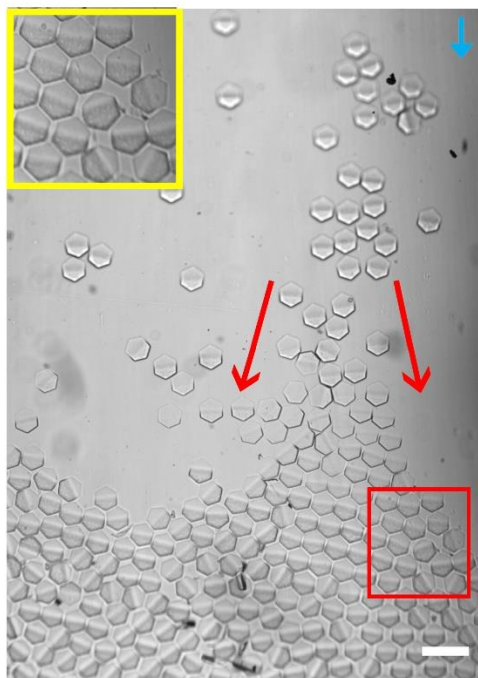


Fig. S4. The irregular distribution of the sliding hexagons along with the sedimentation well width results in their redistribution after reaching the structure (indicated by the red arrows, the blue arrow indicates the sedimentation direction, red rectangle indicates the area depicted in Figure S5, the scale bar corresponds to 200 μm).

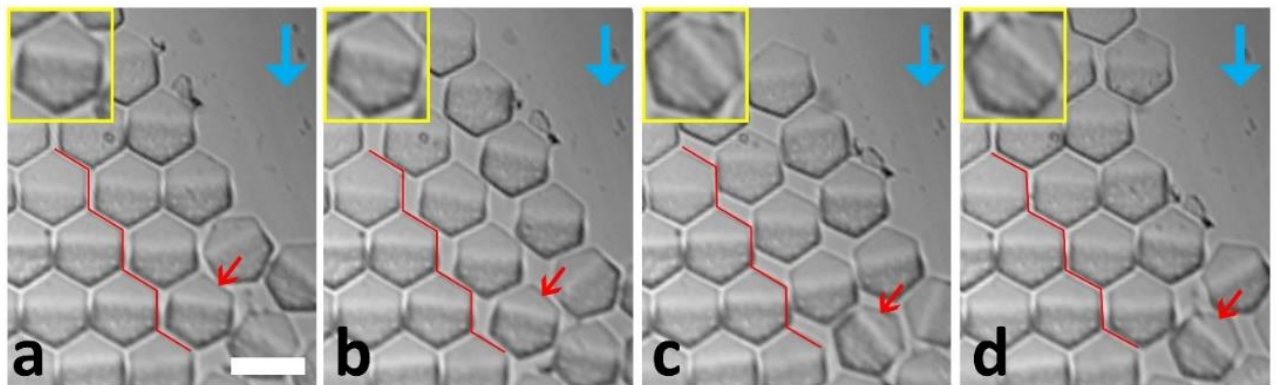


Fig. S5. Orientation loss during building block redistribution near a defect. The red zigzag line indicates the dislocation line; the red arrow highlights the hexagon with the lost orientation. The blue arrow indicates sedimentation direction. The scale bar corresponds to 100 μm .

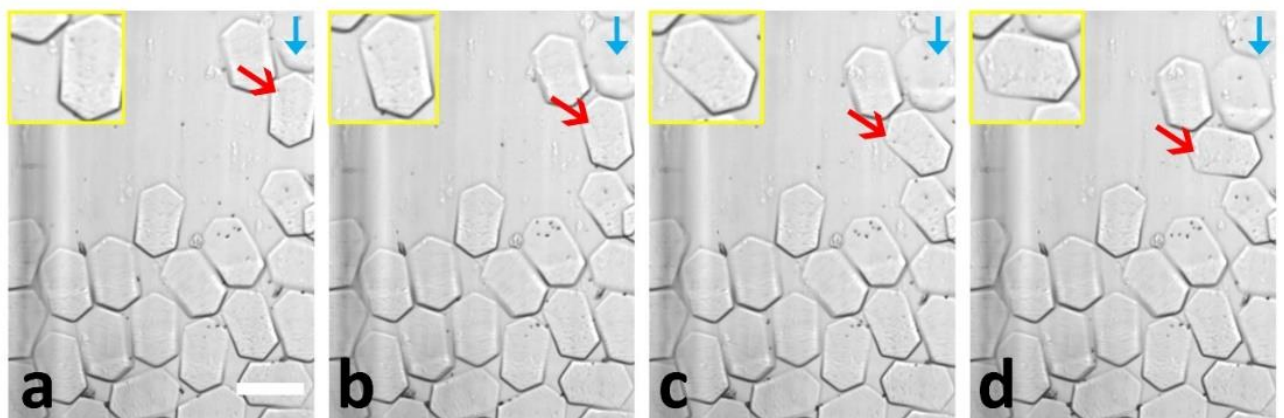


Fig. S6. Error on incorporation due to tipping over of elongated hexagon microgels. The blue arrow indicates sedimentation direction; the scale bar corresponds to 200 μm .

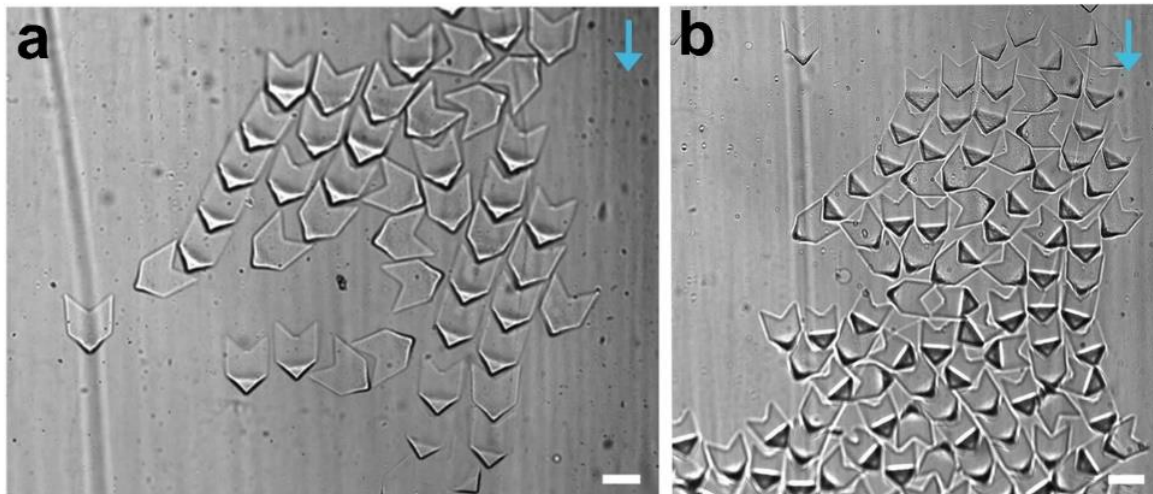


Fig. S7. (a) Interlocked chains of arrow-shaped microgels (b) The V-shaped particle assembly. The blue arrow indicates the sedimentation direction; the scale bar corresponds to 100 μm .

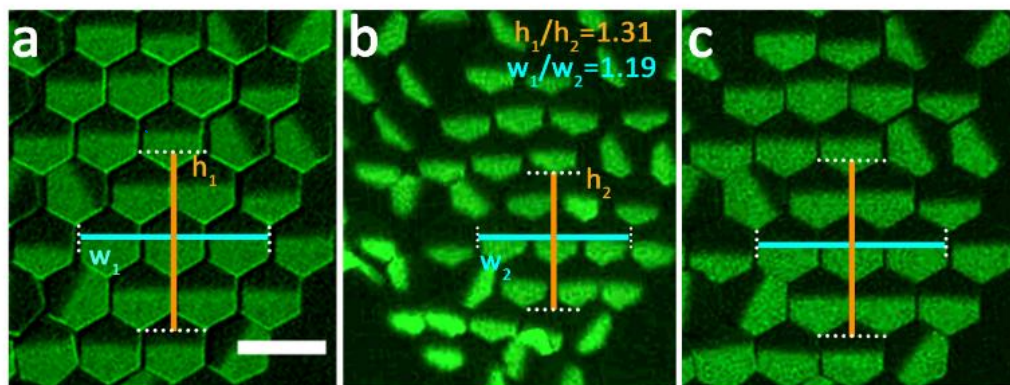


Fig. 9. Anisotropic deformation of microgel sheet, subjected to heating and cooling. (a) 25, (b) 60, (c) 25 $^{\circ}\text{C}$. Scale bar corresponds to 100 μm .

- 1 D. Dendukuri, P. Panda, R. Haghgoie, J. M. Kim, T. A. Hatton and P. S. Doyle, *Macromolecules*, 2008, **41**, 8547–8556.
- 2 I. Hutchings and P. Shipway, *Tribology: Friction and Wear of Engineering Materials*, Butterworth-Heinemann, 2017.
- 3 Y. Du, E. Lo, S. Ali and A. Khademhosseini, *Proc. Natl. Acad. Sci.*, 2008, **105**, 9522–9527.
- 4 Fernandez Javier G. and Khademhosseini Ali, *Adv. Mater.*, 2010, **22**, 2538–2541.
- 5 T. Canal and N. A. Peppas, *J. Biomed. Mater. Res.*, 1989, **23**, 1183–1193.